British Journal of Pharmacology (1999) 128, 1071–1081
http://www.stockton-press.co.uk/bjp

Effects of rupatadine, a new dual antagonist of histamine and platelet-activating factor receptors, on human cardiac Kv1.5 channels

[1]Ricardo Caballero, [1]Carmen Valenzuela, [1]Mónica Longobardo, [1]Juan Tamargo & *,[1]Eva Delpón

[1]Department of Pharmacology, School of Medicine, Universidad Complutense, 28040-Madrid, Spain

1 The effects of rupatadine, a new dual antagonist of both histamine H_1 and platelet-activating factor receptors, were studied on human cloned hKv1.5 channels expressed in Ltk^- cells using the whole-cell patch-clamp technique.

2 Rupatadine produced a use- and concentration-dependent block of hKv1.5 channels ($K_D = 2.4 \pm 0.7$ μM) and slowed the deactivation of the tail currents, thus inducing the 'crossover' phenomenon.

3 Rupatadine-induced block was voltage-dependent increasing in the voltage range for channel opening suggesting an open channel interaction. At potentials positive to +10 mV the blockade decreased with a shallow voltage-dependence. Moreover, rupatadine also modified the voltage-dependence of hKv1.5 channel activation, which exhibited two components, the midpoint of the steeper component averaging -25.2 ± 2.7 mV.

4 When the intracellular K^+ concentration ($[K^+]_i$) was lowered to 25% the voltage-dependent unblock observed at positive potentials was suppressed and the activation curve in the presence of rupatadine did not exhibit two components even when the midpoint of the activation curve was shifted to more negative potentials (-30.3 ± 1.3 mV).

5 On channels mutated on the residue R485 (R485Y) which is located on the external entryway of the pore the rupatadine-induced block did not decrease at potentials positive to +10 mV. In contrast, on V512M channels rupatadine reproduced all the features of the blockade observed on wild type channels.

6 All these results suggest that rupatadine blocks hKv1.5 channels binding to an external and to an internal binding site but only at concentrations much higher than therapeutic plasma levels in man. Efflux of K^+ promotes the unbinding from the external site. Furthermore, rupatadine binds to an internal site and dramatically modifies the voltage-dependence of channel opening.

Keywords: hKv1.5 channels; Ltk^- cells; rupatadine; histamine H_1 receptor antagonist; PAF-antagonist; patch-clamp

Abbreviations: ATP, adenosine triphosphate; ≈, approximately equals; C_{max}, peak plasma concentration; DMEM, Dulbecco's modified Eagle medium; DMSO, dimethyl sulphoxide; EGTA, ethylene glycol-bis (b-amino ethyl ether) tetraacetic acid; pH, hydrogen-ion activity, negative logarithm of (hydrogen-ion exponent); HEPES, N-[2-Hydroxyethyl]piperazine-N′-[2-ethanesulphonic acid]; I-V, current-voltage relationship; k, slope factor for the activation curve; k, apparent association rate constant; $[K^+]_i$, intracellular potassium concentration; K_D, apparent affinity constant; l, apparent dissociation rate constant; n_H, Hill coefficient; PAF, platelet activating factor; PCR, polymerase chain reaction; QA, quaternary ammonium compounds; τ, time constant; τ_{Block}, time constant of development of block; TEA, tetraethylammonium; Tris, 2-amino-2-hydroxymethyl-propan-1,3-diol; V_h, the midpoint of activation curve; V_m, membrane test potential; WT, wild type hKv1.5 channels

Introduction

Histamine and platelet activating factor (PAF) are important mediators released during allergic and inflammatory disorders (Braquet *et al*., 1987; Hanahan, 1986). Histamine H_1-receptor antagonists have long been widely used for the symptomatic relief of allergic and inflammatory diseases (Simons & Simons, 1991). Platelet-activating factor (PAF) antagonists also provide a more recent therapeutic approach in the treatment of allergic and inflammatory disorders (Braquet *et al*., 1987; Koltai *et al*., 1991). PAF and histamine have complementary effects during an allergic response. In fact, histamine has been considered a mediator of the early response (Serafin & Austen, 1987), as it is performed and released from mast cells and has a rapid onset of action (Schwartz, 1994), whereas PAF may account for the later response, as it is synthesized *de novo* (Sciberras *et al*., 1988) and has a slow onset of action (Koltai *et al*., 1991). Moreover, in some cells, one mediator may promote the release of the other (McIntyre *et al*., 1985; Presscott *et al*., 1987). Thus, it may be proposed that the blockade of both histamine and PAF receptors may be of greater clinical effectiveness than the blockade of only one of them (Merlos *et al*., 1997).

Rupatadine fumarate (8-chloro-6,11-dihydro-11-[1-[(5-methyl-3-pyridinyl)methyl]-4-piperidinylidene]-5H-benzo[5,6]-cyclohepta[1,2-b]pyridine) is a long acting dual antagonist of both histamine H_1 and PAF receptors (Carceller *et al*., 1994). In *in vivo* and *in vitro* studies, rupatadine was as potent or even more potent than second generation antihistamines (loratadine, terfenadine and cetirizine) or selective PAF antagonists such as BN-52021 and WBE-2086 (Carceller *et al*., 1994; García Rafanell, 1996; Merlos *et al*., 1997). Very recently it has been demonstrated that the new generation of H_1-receptor

* Author for correspondence; E-mail: edelpon@eucmax.sim.ucm.es

antagonists blocked several cardiac K^+ currents (Berul & Morad, 1995; Crumb *et al*., 1995; Salata *et al*., 1995; Delpón *et al*., 1999b). Moreover, it has been also shown that they blocked hKv1.5 channels cloned from human heart and expressed in mammalian cell lines (Rampe *et al*., 1993; Delpón *et al*., 1997; Lacerda *et al*., 1997; Valenzuela *et al*., 1997). These later channels are the counterpart of the ultrarapid delayed rectifier current which is involved in the control of the duration of the atrial action potentials in the human heart (Wang *et al*., 1993).

Thus, the present study was undertaken to analyse whether rupatadine modifies hKv1.5 channels and to compare its effects with those previously reported with other non-sedating H_1-receptors antagonists.

Methods

Cell culture

Wild-type and site-directed mutated hKv1.5 channels were stably expressed in mouse L-cell line using procedures previously described elsewhere (Snyders *et al*., 1993; Yeola *et al*., 1996; Franqueza *et al*., 1997). Briefly, point mutations were generated by a method involving the polymerase chain reaction (PCR), and all PCR-generated sequences were verified directly by double-stranded sequencing. Once the desired sequence was confirmed, the complete coding sequence was ligated into the pMSVneo expression vector, used for stable transfection into Ltk^- cells as described elsewhere (Snyders *et al*., 1993; Yeola *et al*., 1996; Franqueza *et al*., 1997). Transfected cells were cultured in DMEM supplemented with 10% horse serum and 0.25 mg ml^{-1} G418 (GIBCO). Prior to experimental use, cultures were incubated with 2 μM dexamethasone for 24 h as expression of the channel was under control of a dexamethasone-inducible promoter (Snyders *et al*., 1992).

Electrical recording

Cells were superfused with an external solution containing (mM): NaCl 130, KCl 4, $CaCl_2$ 1, $MgCl_2$ 1, HEPES 10 and glucose 10; (pH = 7.4 with NaOH). Recording pipettes were filled with an 'internal' solution containing (mM): K-aspartate 80, KCl 42, KH_2PO_4 10, MgATP 5, phosphocreatine 3, HEPES 5 and EGTA 5 (pH = 7.2 with KOH). In some experiments the intracellular K^+ concentration ($[K^+]_i$) was lowered to 25% by the equimolar substitution of K-aspartate by TrisCl. Rupatadine was initially dissolved in dimethyl sulphoxide to yield 0.1 M stock solutions. Further dilutions were carried out in external solution to obtain the desired final concentrations. DMSO did not affect the current at concentrations up to 0.1%.

hKv1.5 currents were measured using the whole-cell configuration of the patch-clamp technique. Recordings were performed at 24–25°C using Axopatch-200B patch-clamp amplifiers and pCLAMP 6.1 software (Axon Instruments). Borosilicate pipettes used had a tip resistance of 1.5–2.5 MΩ when filled with the internal solution and immersed in the external solution. The capacitive transients elicited by symmetrical 10 mV steps from −80 mV were recorded for subsequent calculation of capacitive surface area, access resistance and input impedance. Maximum outward current amplitudes at +60 mV averaged 1.4 ± 0.1 nA, mean uncompensated access resistance was 3.3 ± 0.5 MΩ and cell capacitance 11.2 ± 0.9 pF (n = 20). Thereafter, capacitance and series resistance compensation were optimized and ≈80% compensation was usually obtained. Thus, no significant voltage errors (< 5 mV) due to uncompensated series resistance were expected. Voltage-clamp command pulses were generated by a 12-bit digital-to-analogue converter. The current records were sampled at 3–10 times the antialias filter setting.

Pulse protocols and analysis

The holding potential was maintained at −80 mV and the cycle time for any protocol was 10 s to avoid accumulation of block. The protocol to obtain current-voltage (I-V) relationships and activation curves consisted of 500 ms pulses that were imposed in 10 mV increments between −80 mV and +60 mV, with additional interpolated pulses to yield 5 mV increments between −30 and +10 mV (activation range of hKv1.5). The 'steady-state' I-V relationships were obtained by plotting the current level after 500 ms as a function of the membrane potential. Between −80 and −40 mV, only passive linear leak was observed and least squares fits to these data were used for passive leak correction. Deactivating 'tail' currents were recorded on return to −40 mV. The activation curve was constructed by plotting the tail current amplitude values elicited on return to −40 mV after 500 ms depolarizations to various test potentials (from −80 to +60 mV) as a function of the membrane potential.

Activation curve for each individual experiment has been fitted with a Boltzmann distribution according to the following equation:

$$y = A/\{1 + \exp[(V_h - V_m)/k]\} \quad (1)$$

where A is the amplitude term, V_h is the midpoint of activation (in mV), V_m is the test potential and k represents the slope factor for the activation curve (in mV). Thereafter, the mean value for V_h and k values for each group of experiments was calculated. Under some circumstances a Boltzmann distribution with two terms was needed to fit the experimental data, the equation being:

$$y = A_1/\{1 + \exp[(V_{h1} - V_m)/k_1]\} + A_2/\{1 + \exp[(V_{h2} - V_m)/k_2]\} \quad (2)$$

To describe the time course of the tail currents upon repolarization exponential analysis was used as an operational approach, fitting the tail currents to an equation of the form:

$$y = C + A_1\exp(-t/\tau_1) + A_2\exp(-t/\tau_2) + \ldots + A_n\exp(-t/\tau_n)$$

where τ_1, τ_2 and τ_n are the system time constants, A_1, A_2 and A_n are the amplitudes of each component of the exponential, and C is the baseline value. The Chebyshev transform and Simplex least-squares algorithm provided in CLAMPFIT (pCLAMP 6.1) and costumer made programs (Dr D. Snyders) were used for the exponential fitting. This curve fitting procedure used a nonlinear least-squares (Gauss-Newton) algorithm; results were displayed in linear and semilogarithmic format, together with the difference plot. Goodness of fit was judged by the χ^2 criterion and by inspection for systematic nonrandom trends in the difference plot.

Fractional block was defined as:

$$f = 1 - I_{Drug}/I_{Control}$$

To describe drug-channel interaction we selected the most common model in which the drug molecule (D) interacts with the receptor (R) in a reversible bimolecular reaction with the formation of a drug-receptor complex (DR). This situation is described by a second order reaction between a ligand or drug (D) and a receptor (R):

$$D + R \underset{l}{\overset{k}{\rightleftharpoons}} DR \quad (3)$$

At the equilibrium:

$$[D][R]/[DR] = K_D = l/k.$$

A reaction described by this model obeys simple mass action principles (Weiland & Molinoff, 1981). Thus, apparent affinity constant, K_D, and Hill coefficient, n_H, were obtained from fitting the fractional block, f, at various drug concentrations [D] to the equation:

$$f = 1/\{1 + (K_D/[D])^{n_H}\} \quad (4)$$

Apparent rate constants for association (k) and dissociation (l) were obtained from fitting:

$$1/\tau_{Block} = k \times [D] + l \quad (5)$$

in which τ_{Block} is the time constant of development of block.

Statistical methods

Data obtained after drug exposure were compared with those obtained under control conditions in a paired manner. For comparisons at a single voltage or drug concentration differences were analysed using the Student's t-test. To analyse block at multiple voltages or drug concentrations, two-way analysis of variance was used. Results are expressed as mean ± s.e.mean. A P-value of less than 0.05 was considered significant.

Results

Concentration-dependent hKv1.5 block

The effect of rupatadine infusion or removal on hKv1.5 currents was monitored with 250 ms-test pulses from −80 mV to +60 mV applied every 30 s. hKv1.5 currents rose rapidly to a peak ($\tau = 1.7 \pm 0.1$ ms, $n = 9$) with a sigmoidal time course and then declined slowly since these channels exhibited slow and partial inactivation (Snyders *et al*., 1993). Figure 1 shows examples of hKv1.5 currents recorded in the absence and 4 min after perfusion of 0.1 μM rupatadine. In all the experiments at the beginning of the infusion rupatadine increased the amplitude of hKv1.5 currents over the whole duration of the depolarizing pulse, this increase averaging 8.2 ± 1.4% ($n = 5$). Thereafter, the current amplitude slowly declined until a new steady-state level was achieved (within 10 min). Figure 2 shows superimposed hKv1.5 currents in control conditions and in the presence of 1 μM rupatadine. Currents were elicited by applying 500-ms pulses from −80 to +60 mV in 20 mV steps. Exposure to 1 μM rupatadine did not modify the activation time course, and slightly decreased the peak current and increased the current decline during the pulse. These results suggest that the inhibition of hKv1.5 current only developed after channels became open. Blocking effects of rupatadine were largely reversible upon washout for 10 min.

Rupatadine reduced the steady-state currents in a concentration-dependent manner (Figure 3a). The reduction of current after 500 ms at +60 mV was used as an index of block. A nonlinear least-squares fit of the concentration-response equation (eq. 4 in Methods) to the individual data points yielded an apparent K_D of 2.4 ± 0.7 μM and a Hill coefficient (n_H) of 0.7 ± 0.1. A fit of the same data with the n_H fixed at 1 (dashed line in Figure 3a), led to an K_D value of 2.3 ± 0.6 μM. These results suggest that binding of rupatadine to hKv1.5

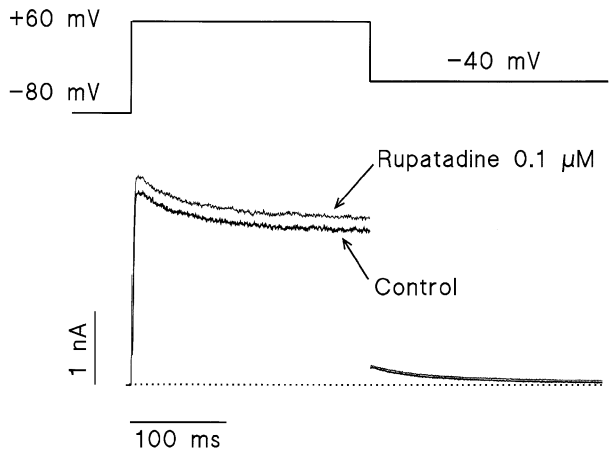

Figure 1 Effects of 0.1 μM rupatadine on hKv1.5 currents recorded 4 min after beginning infusion of the drug. hKv1.5 currents were elicited by applying 250 ms pulses to +60 mV from a holding potential of −80 mV. Data filtered at 2 kHz and digitized at 10 kHz. The dotted line represents the zero current level.

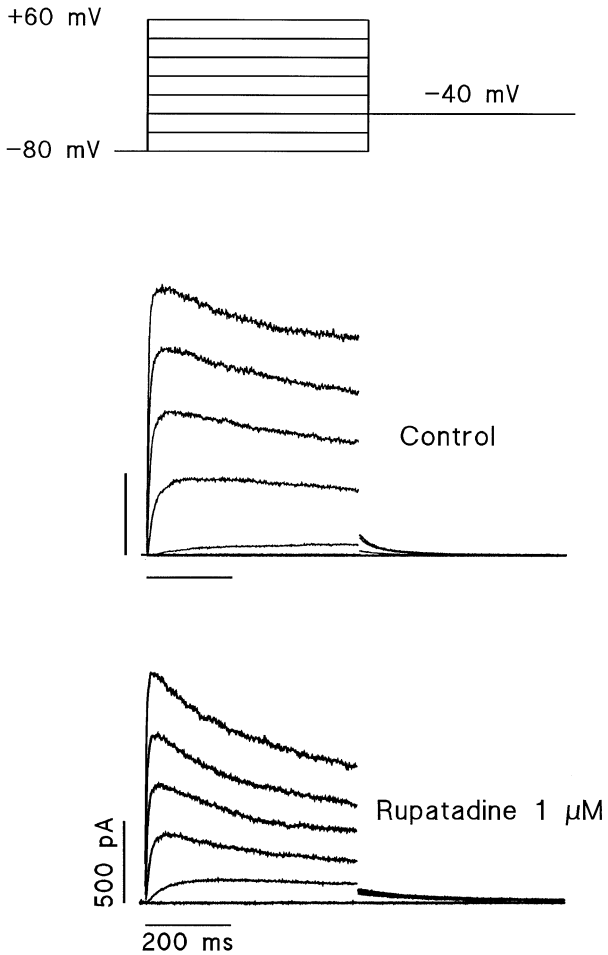

Figure 2 Steady-state effects of 1 μM rupatadine on hKv1.5 currents. Superimposed current traces are shown for 500 ms depolarizing pulses from −80 mV to voltages between +60 to −80 mV in 20 mV steps (voltage protocol is shown on top) in the absence (control) and in the presence of rupatadine. Data filtered at 1 kHz and sampled at 2 kHz.

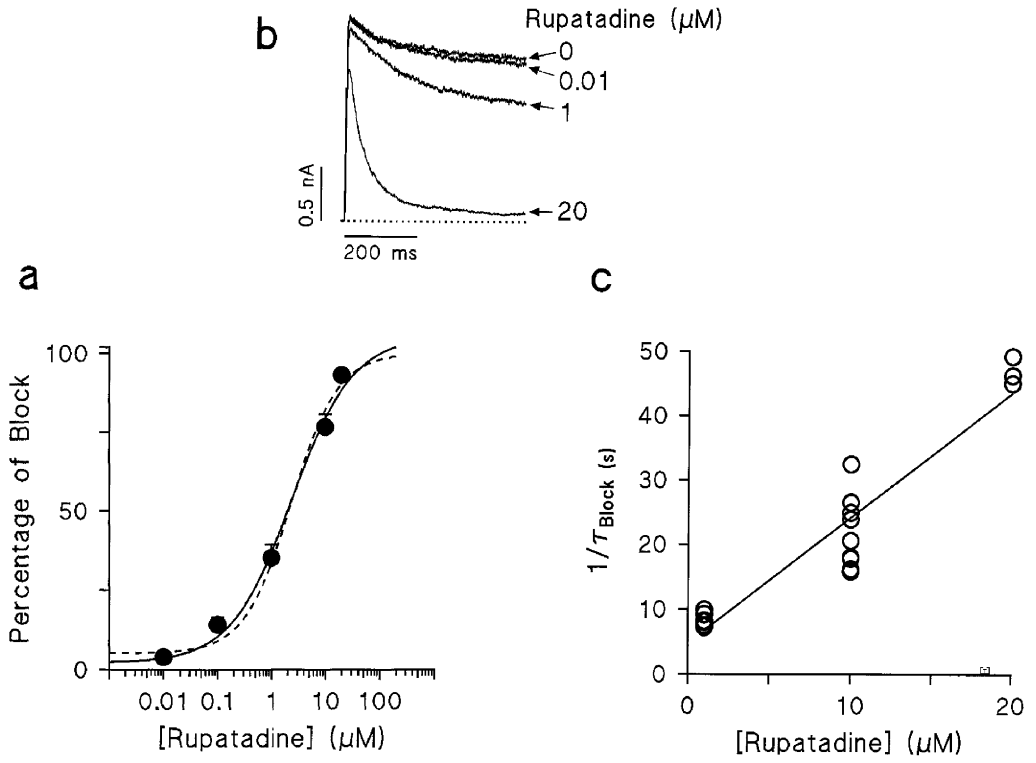

Figure 3 (a) Concentration-dependence of rupatadine-induced block of hKv1.5 currents. Reduction of current (relative to control) after 500 ms depolarizations to +60 mV was used as index of block. The continuous line represents the fit of the experimental data to eq. 4 (see Methods). The dashed line represents the fit to the same data with the Hill coefficient fixed at 1. Each point represents the mean±s.e.mean of 4–8 experiments. (b) Superimposed hKv1.5 current traces obtained by applying 500 ms pulses to +60 mV in the absence (0) and in the presence of rupatadine 0.01, 1 and 20 μM. The dotted line represents the zero current level. (c) Plot of the inverse of the time constant of block ($1/\tau_{Block}$) as a function of the rupatadine concentration. The time constant of the fast component of decline of hKv1.5 currents ins: (τ_{Block}) was obtained from biexponential fits of the falling phase of the current traces. The solid line represents the fit to eq. 5 (see Methods) from which the apparent association (k) and dissociation rate (*l*) constants were calculated.

channels is a simple bimolecular reaction that follow eq. 3 in Methods.

Figure 3b shows superimposed outward currents recordings elicited by 500-ms pulses to +60 mV in the absence (0) and in the presence of increasing rupatadine concentrations (0.01, 1 and 20 μM). As it is shown rupatadine induced a concentration-dependent increase in the rate of decline of the currents during the depolarization. Current decay was fitted by a double exponential function, comprised of a fast and a slow component. The slow time constant (260±15.4 ms) reflects the slow and partial inactivation elicited under these conditions. At drug concentrations higher than 1 μM, the fast time constant was at least 10 times faster than the slow inactivation and was considered as a good approximation of the time constant of development of block. Figure 3c shows the plot of the $1/\tau_{Block}$ vs the rupatadine concentration for data obtained in 15 experiments. The straight line is the least-squares fit to eq. 5 in Methods. Slope and intercept with the ordinate axis for the fitted relation yielded an apparent association (k) and dissociation (*l*) rate constants of $(1.9\pm0.1)\times10^6$ $M^{-1}s^{-1}$ and 4.8 ± 1.6 s^{-1}, respectively. Furthermore, the K_D ($=l/k$) value derived from this relationship for hKv1.5 block was 2.5 μM. Thus, K_D values determined kinetically and by Hill analysis are almost identical suggesting that rupatadine-induced block of hKv1.5 channels is the result of its binding following a simple bimolecular reaction.

To further characterize the time-dependent effects of rupatadine on hKv1.5 channels, its effects on the time course of tail current decline were also analysed. Figure 4 shows superimposed tail currents elicited on return to −40 mV after 500-ms pulses to +60 mV. In control conditions the deactivation process mainly reflects the irreversible closing of the channels at negative potentials, and was fitted to a monoexponential function, the time constant of deactivation averaging 53.9±6.8 ms ($n=8$). However, as it is represented in the typical experiment shown in Figure 4, in the presence of 1 μM rupatadine the peak tail current amplitude decreased and the subsequent time course of the tail current was slowed, so that the calculated time constant of deactivation increased to 116.3±19.9 ms ($P<0.01$). As a consequence of the slowing a crossing of the tail currents was observed (i.e. the 'crossover phenomenon').

Voltage dependence of rupatadine induced block

Figure 5a shows the current-voltage relationships (I-V curves) obtained in the absence and in the presence of 1 μM rupatadine. The I-V curves were obtained by plotting the current amplitude at the end of the depolarizing pulse as a function of the membrane potential. Rupatadine reduced hKv1.5 current over the whole range over which the current is activated. To quantify the effects of the voltage on the drug-channel interaction in Figure 5b the relative current (I_{RUP}/I_{CON}) was plotted as a function of the membrane potential together with the mean activation curve obtained under control conditions (dotted line). It can be observed that the blockade reached a maximum at +10 mV and thereafter it decreased with a shallow voltage-dependence. In fact, the

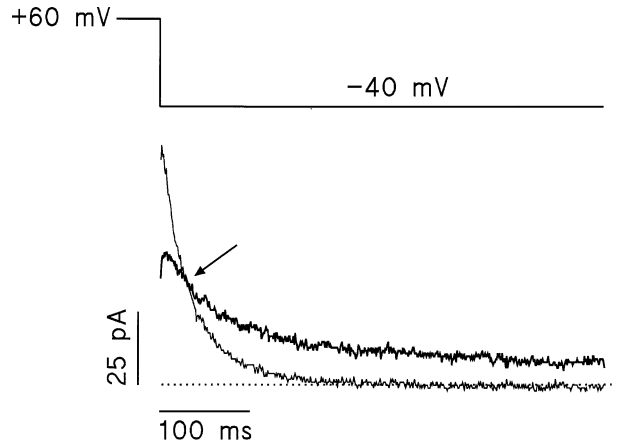

Figure 4 Effects of 1 μM rupatadine on the tail currents elicited on return to −40 mV after pulses to +60 mV (voltage protocol is shown on top). The arrow indicates the tail current crossover. Data filtered at 1 kHz and sampled at 2 kHz. The dotted line represents the zero current level.

rupatadine-induced block at +10 mV was significantly higher than that obtained at +60 mV (46.2±1.3% vs 37.8±1.4%, $n=9$, $P<0.05$). This voltage-dependence cannot be attributed to the effects of the transmembrane electrical field on the interaction between the charged form of the drug and the receptor at the channel level since rupatadine predominates in its neutral form at physiological pH. Further analysis of the voltage-dependence of hKv1.5 channel activation revealed that rupatadine dramatically modified this process. Figure 5c shows the activation curves in the absence and the presence of drug obtained by plotting the peak tail current amplitude as a function of the membrane potential. Under control conditions the activation curve was obtained fitting a Boltzmann distribution (eq. 1 in Methods) to the experimental data. The averaged values for V_h and k values in the absence of drug were −16.5±2.0 mV and 4.5±0.3 mV ($n=6$), respectively. In the presence of rupatadine, the activation curve of hKv1.5 channels displayed two components. The first steeper component was responsible for ≈75% of the activation process and was followed by a shallow component. The solid line illustrates a fit of experimental data with a sum of two Boltzmann components (eq. 2 in Methods). Rupatadine significantly shifted the V_h value of the steeper component to more negative potentials ($V_h=-25.2\pm2.7$ mV, $P<0.01$), without altering the k value (3.7±0.5 mV). The V_h of the shallow component ($k=39.6\pm5.5$ mV) averaged 97.2±11.0 mV indicating that in the presence of rupatadine activation did not reach saturation over the range of membrane potentials tested.

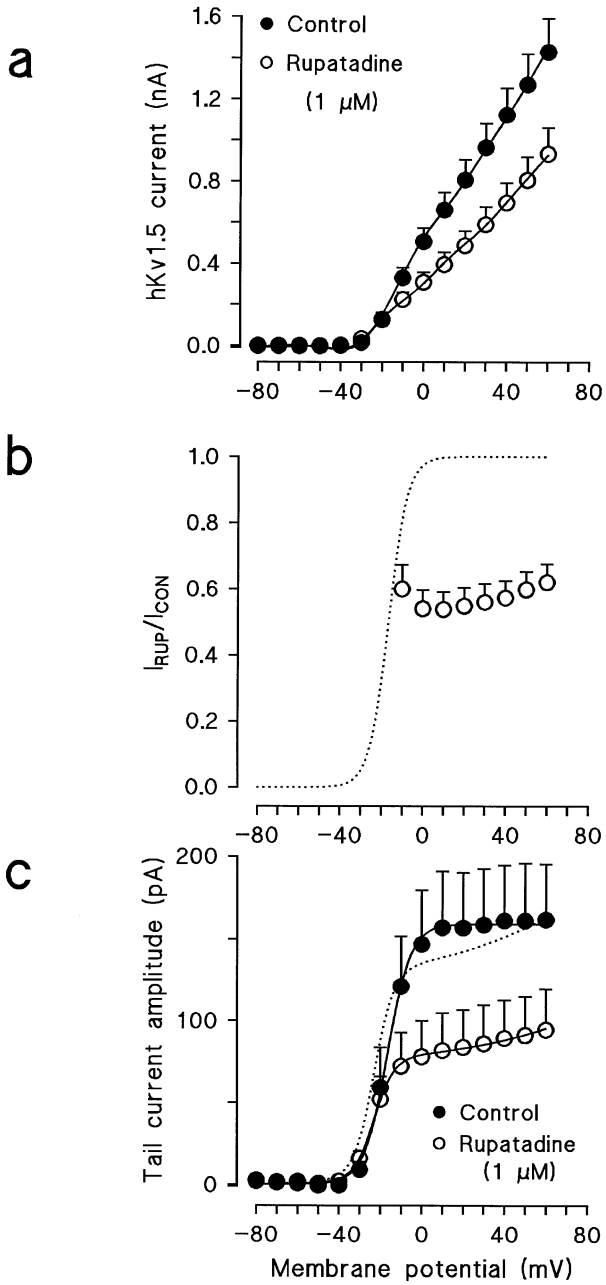

Figure 5 (a) Current voltage relationships (500 ms isochronal) of hKv1.5 channels in the absence and in the presence of 1 μM rupatadine. (b) Fractional block ($f=I_{RUP}/I_{CON}$) from data shown in panel a. The dotted line represents the mean activation curve in control conditions. (c) Effects of 1 μM rupatadine on the voltage-dependence of hKv1.5 channel activation. Activation curve in the absence of drug was fitted with a single Boltzmann component (continuous line, eq. 1, Methods), while in the presence of rupatadine it was fitted with a sum of two components (solid line, eq. 2 in Methods). Dotted line represents the activation curve in the presence of rupatadine scaled to control values to better show the shift in the activation curve. Each point represents the mean±s.e.mean of nine experiments.

Use-dependent effects of rupatadine on hKv1.5 channels

To analyse the possible use-dependence of block, in the next group of experiments trains of 200 ms-pulses to +10 or +60 mV at 2 Hz were applied. Trains of stimuli were separated from each other by 2 min intervals. Figure 6a shows original current records obtained in a cell when applying trains of pulses in the absence and in the presence of 1 μM rupatadine. Under control conditions current amplitude decreased by 22.3±2.3% ($n=10$) during the application of the trains to +10 mV and to +60 mV as a consequence of the accumulation of the slow inactivation. Figure 6b shows the ratio of current amplitudes in the absence and in the presence of rupatadine during application of the trains. It can be observed that a certain amount of block was apparent from the first depolarization applied (i.e., 'tonic block') which averaged 16.5±5.0% and 13.5±5.6% at +10 and +60 mV, respectively ($n=5$). Thereafter, during application of the train the blockade increased until a new steady-state level was reached, i.e. the rupatadine-induced block was use-dependent, aver-

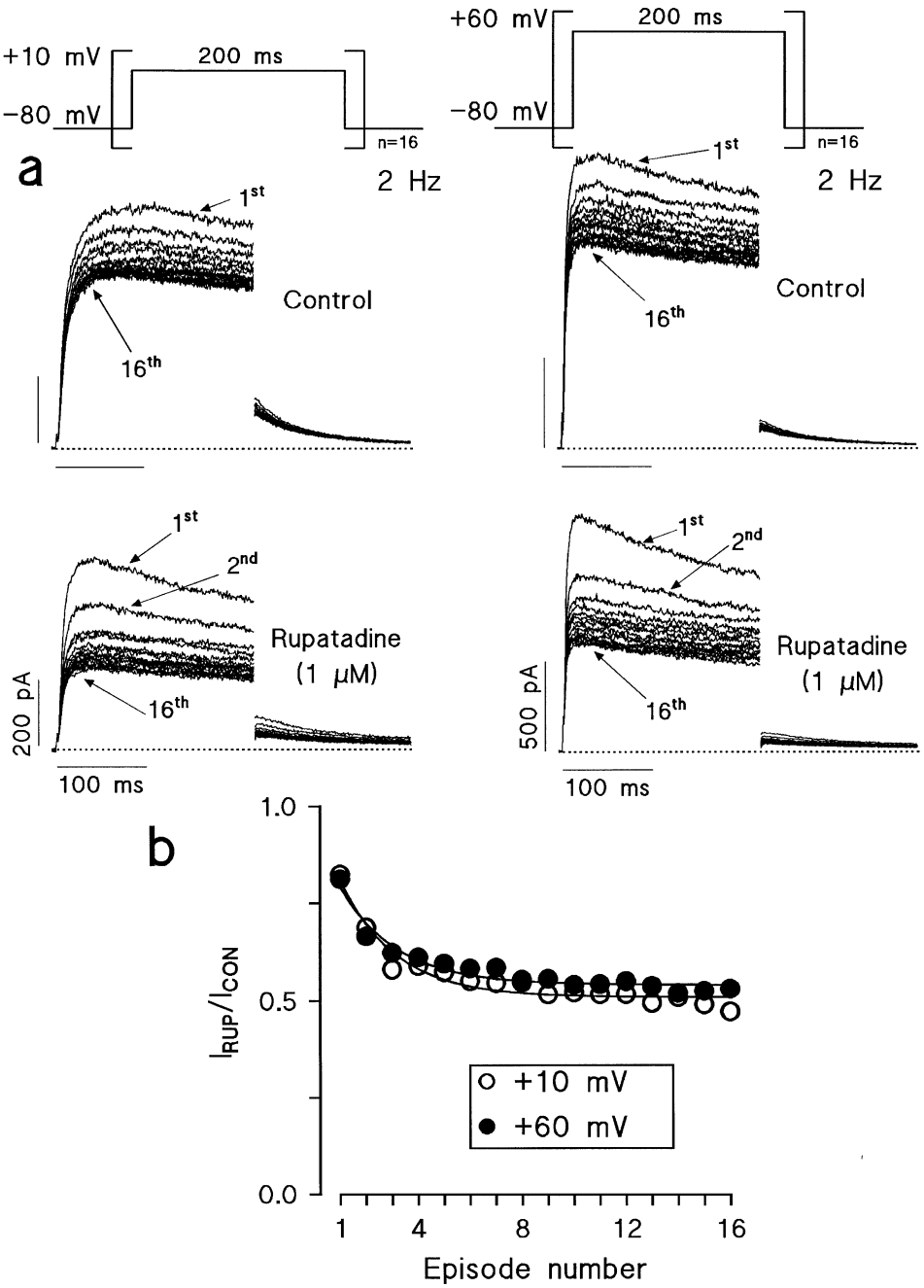

Figure 6 (a) Frequency-dependent effects of 1 μM rupatadine on hKv1.5 currents. Original current records obtained when applying trains of 200-ms pulses to +10 mV (left panel) and to +60 mV (right panel) at 2 Hz in the absence and in the presence of rupatadine. (b) Plot of the ratio of the amplitude of the current in the presence and in the absence of rupatadine when trains of pulses to +10 or to +60 mV at 2 Hz were applied as a function of the number of pulses. Continuous lines represent the best monoexponential fits of the data.

aging 53.2±3.2% and 46.5±4.2% ($n=5$, $P<0.01$) when trains of pulses to +10 or to +60 mV were applied, respectively. The onset kinetics of the use-dependent block was analysed by fitting to a monoexponential function the relative current against the number of consecutive pulses of the trains (continuous lines in Figure 6b). Steady-state frequency dependent block was achieved between the second and the third pulse of the train and thus, the rate constant of the onset kinetics when trains of pulses at 2 Hz to +10 or to +60 mV were applied yielded 0.49±0.1 pulse^{-1} and 0.61±0.1 pulse^{-1}, respectively.

Time- and use-dependent effects of rupatadine on hKv1.5 channels suggest an open channel interaction. In fact, drug-induced blockade increased in the voltage range of channel opening. These results suggest that blocking effects of rupatadine resemble those previously described with other positively charged antiarrhythmics (Snyders *et al*., 1992; Valenzuela *et al*., 1996), local anaesthetics (Franqueza *et al*., 1997; Longobardo *et al*., 1998) and antihistamines (Valenzuela *et al*., 1997; Caballero *et al*., 1997) drugs. However, and in contrast to the blockade produced by all these drugs, at positive potentials a voltage-dependent unblock was observed. Thus, the next groups of experiments were developed with the goal to elucidate the mechanisms of the voltage-dependent effects of rupatadine.

Effects of rupatadine at low intracellular $[K^+]_i$

To test whether the reduction in the $[K^+]_i$ modifies the effects of rupatadine, the $[K^+]_i$ was decreased to 25%. Figure 7a shows the I-V relationships obtained under these conditions in the absence and in the presence of 1 μM rupatadine. At negative potentials ($-40/-30$ mV) rupatadine slightly increased the current amplitude, whereas it decreased hKv1.5 currents at potentials positive to -20 mV. In fact, the rupatadine-induced block at $+60$ mV was not different from that obtained at normal $[K^+]_i$ ($31.5\pm3.8\%$, $n=6$, $P>0.05$). However, the reduction of the $[K^+]_i$ suppressed the voltage-dependent unblock observed at potentials positive to $+10$ mV. This is shown in Figure 7b, where the relative current was plotted as a function of the membrane potential. In this group of experiments the blockade obtained at $+10$ mV averaged $32.8\pm4.9\%$ ($n=6$, $P>0.05$). Figure 7c shows the activation curve in the absence and in the presence of 1 μM rupatadine. Under control conditions the V_h and k values averaged -21.0 ± 0.6 mV and 3.3 ± 0.1 mV ($n=6$), respectively. Rupatadine shifted the midpoint of the activation curve to more negative potentials (-30.3 ± 1.3 mV, $P<0.05$), whereas it did not modify the slope factor (3.8 ± 0.5 mV). More, interestingly at low $[K^+]_i$ the activation curve of hKv1.5 channels in the presence of rupatadine did not become biphasic.

Effects of rupatadine on mutant channels

It has been described that residue at position 449 on *Shaker* channels determines important functional properties, such as external tetraethylammonium sensitivity (MacKinnon & Yellen, 1990) and C-type inactivation rate (López-Barneo *et al*., 1993). Wild-type hKv1.5 channels (WT) at the equivalent position (485) present arginine, and thus, firstly we studied whether the mutation R485Y affected rupatadine-induced block. Figure 8a shows superimposed currents recordings elicited by 500-ms pulses to $+60$ mV in the absence and in the presence of 1 μM rupatadine. As it can be observed, rupatadine increased the current decline during depolarization and inhibited by $34.9\pm3.0\%$ hKv1.5 currents at the end of the pulse. Moreover, it also slowed the time course of tail current decline from 48.6 ± 9.2 ms to 103.8 ± 12.7 ms ($n=5$, $P<0.05$). Voltage-dependence of activation of R485Y mutant channels was similar to that of WT channels, the V_h and the k values averaging -16.5 ± 2.8 mV and 4.8 ± 0.4 mV ($n=5$), respectively. As it is shown in Figure 8b, in the presence of rupatadine R485Y channel activation became biphasic and similarly to that observed in WT channels, it shifted the V_h of the steeper component ($k=4.0\pm0.2$ mV) to more negative potentials (-27.8 ± 4.4 mV, $n=5$, $P<0.01$), while the V_h of the shallow component averaged 111.4 ± 10.7 mV. Figure 8c shows the relative current amplitude as a function of the membrane potential. The results indicated that at voltages at which the activation curve reached saturation in the absence of drug (>0 mV) the blockade of R485Y channels was voltage-independent. In fact, the blockade at $+10$ mV was similar to that obtained at $+60$ mV ($34.7\pm4.4\%$, $n=5$, $P>0.05$).

We also studied the effects of rupatadine on V512M channels since it has been demonstrated that this residue is involved in the internal binding site of bupivacaine, a tertiary amine local anaesthetic (Franqueza *et al*., 1997). This mutation dramatically affected the voltage-dependence of channels activation. In fact, in these channels the V_h value of the activation curve was shifted in the hyperpolarizing direction averaging -53.0 ± 1.1 mV ($n=4$). Thus, in this group of experiments the holding potential was -100 mV and 500-ms pulses from -100 to $+40$ mV were applied. Figure 8d shows superimposed currents recordings elicited by pulses to $+40$ mV in the absence and in the presence of 1 μM rupatadine. Figure 8e shows the I-V curves obtained in the absence and in the presence of 1 μM rupatadine. Rupatadine-induced block of V512M channels at $+40$ mV averaged $40.9\pm6.0\%$ ($n=4$) and similarly to what was observed on WT channels was voltage-dependent. Figure 8f illustrates that the blockade significantly decreased as a function of the membrane potential, averaging $63.7\pm9.2\%$ ($n=4$, $P<0.01$) at -30 mV.

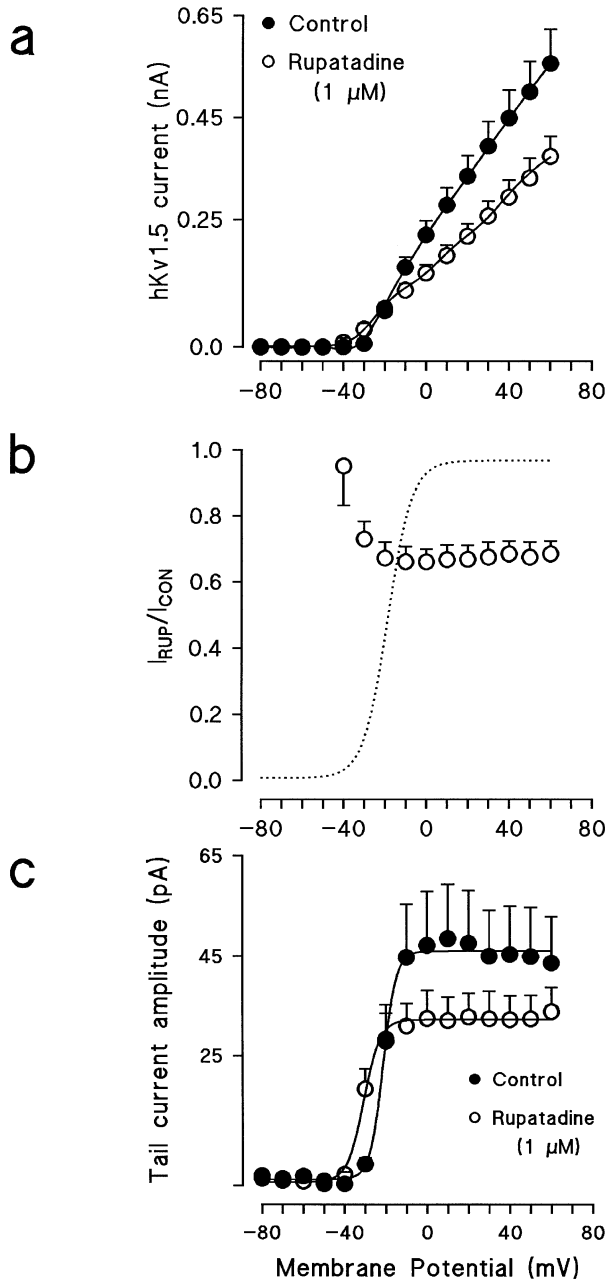

Figure 7 Effects of 1 μM rupatadine at low $[K^+]_i$. (a) Current voltage relationship (500 ms isochronal) of hKv1.5 channels in the absence and in the presence of 1 μM rupatadine. (b) Fractional block ($f=I_{RUP}/I_{CON}$) from data shown in panel a. The dotted line represents the mean activation curve in control conditions. (c) Effects of 1 μM rupatadine on the voltage-dependence of hKv1.5 channel activation. Activation curve in the absence and in the presence of drug were fitted with a single Boltzmann component (continuous line, eq. 1, Methods). Each point represents the mean$\pm$s.e.mean of six experiments.

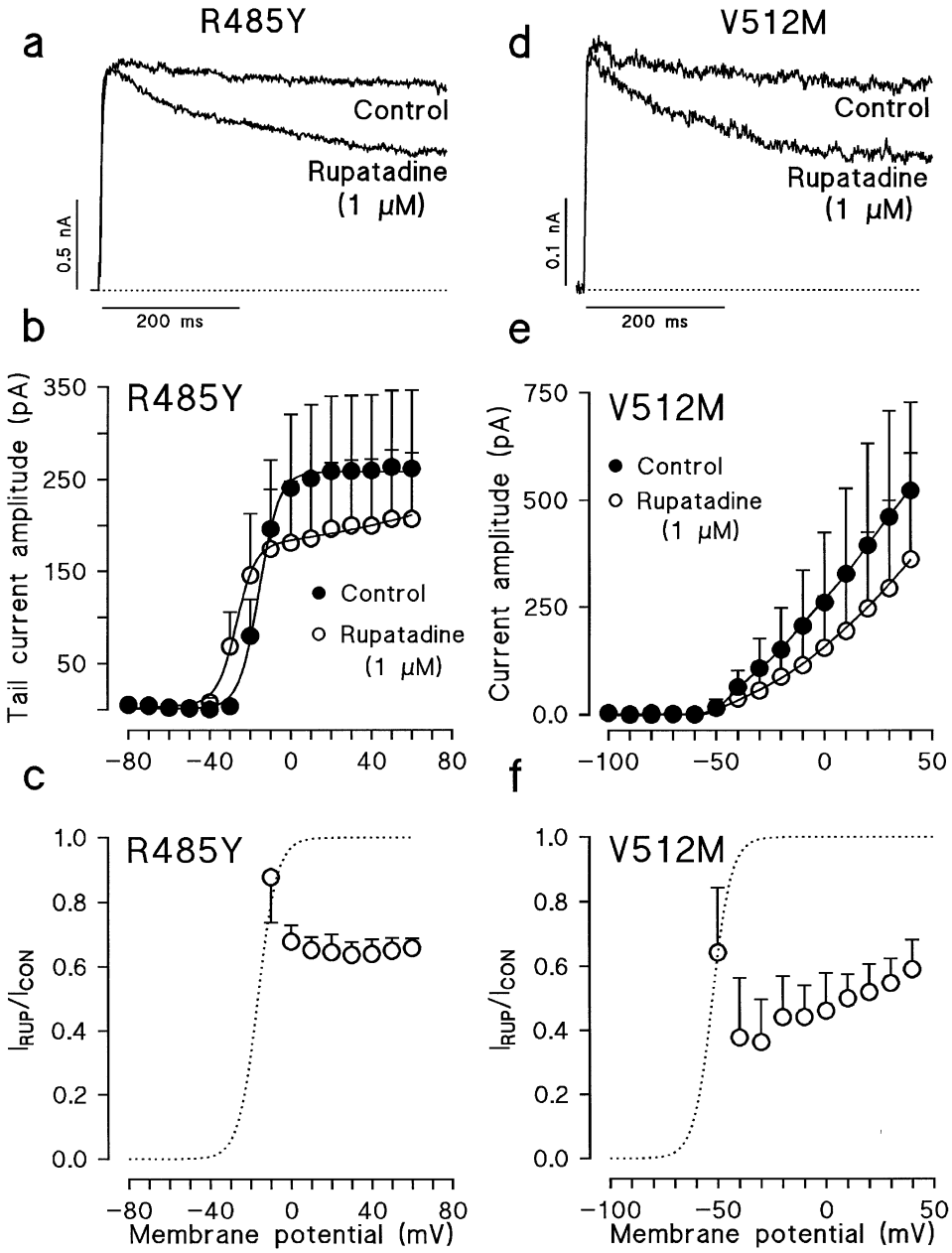

Figure 8 (a) Effects of 1 μM rupatadine on R485Y channels. Superimposed current traces are shown for 500 ms depolarizing pulses from -80 mV to $+60$ mV in the absence (control) and in the presence of rupatadine. (b) Effects of 1 μM rupatadine on the voltage-dependence of R485Y channels activation. Activation curve in the absence of drug was fitted with a single Boltzmann component (continuous line, eq. 1, Methods), while in the presence of rupatadine was fitted with a sum of two components (solid line, eq. 2 in Methods). (c) Fractional block ($f = I_{RUP}/I_{CON}$) induced by 1 μM rupatadine on R485Y channels plotted as function of the membrane potential. (d) Effects of 1 μM rupatadine on V512M channels. Superimposed current traces are shown for 500 ms depolarizing pulses from -100 mV to $+40$ mV in the absence (control) and in the presence of rupatadine. (c) Current voltage relationship (500 ms isochronal) of V512M channels in the absence and in the presence of 1 μM rupatadine. (f) Fractional block ($f = I_{RUP}/I_{CON}$) from data shown in panel e induced by 1 μM rupatadine on V512M channels plotted as function of the membrane potential. The dotted line in panels a and d represents the zero current level. The dotted line in panels c and f represents the mean activation curve in control conditions. In panels b and c, each point represents the mean $\pm$ s.e.mean of five experiments. In panels e and f each point represents the mean $\pm$ s.e.mean of four experiments.

Discussion

The present results demonstrated that rupatadine blocked in a concentration-, time- and voltage-dependent manner hKv1.5 channels. Rupatadine is a potent orally active and long-lasting histamine (H_1) and PAF receptor antagonist (Merlos *et al.*, 1997). The peak plasma concentration (C_{max}) achieved in healthy volunteers after oral administration of 20 mg per day (the highest therapeutical dose) was 5.5 nM (García Rafanell, 1996). These results indicated that these C_{max} values were almost 400 fold below the K_D for hKv1.5 block in the present study. Therefore, a proarrhythmic effect of rupatadine due to a blockade of this human K^+ channel is not expected.

Rupatadine increases the hKv1.5 current

At low concentrations, rupatadine transiently increased the hKv1.5 currents elicited at membranes potentials at which activation of hKv1.5 channels reached saturation. Thus, this effect cannot be the consequence of a shift in the voltage-

dependence of channel activation induced by the drug. A similar increase in the current amplitude at these positive voltages has been observed with losartan, and its metabolite E3174, two angiotensin II type 1 receptor antagonists (Delpón *et al*., 1998) and with benzocaine (Delpón *et al*., 1999a). The molecular mechanism underlying this unexpected effect is unknown and needs to be studied in more detail at the single channel level. However, similar effects were previously described with almokalant, a selective K^+ channel blocker in rabbit ventricular myocytes (Carmeliet, 1993), and with a quaternary analogue of quinidine (Q^+1C) on Kv1.2 channels (Tseng *et al*., 1996) but only at 100 fold higher concentrations than those reported in this paper with rupatadine.

Voltage-dependent effects of rupatadine on hKv1.5 channels

Time-dependent block induced by rupatadine exhibited similar characteristics to those previously reported for antiarrhythmics (Snyders *et al*., 1992; Valenzuela *et al*., 1996) and tertiary amine local anaesthetics on hKv1.5 channels (Franqueza *et al*., 1997; Longobardo *et al*., 1998). Rupatadine induced a decline of the current during the application of the depolarizing pulse which reflected the transition to a channel state with a higher affinity for the drug (C→O). Moreover, it decreases the rate of decay of the tail and induces a crossover phenomenon, indicating that drug unbinding is required before channels can close. Finally, rupatadine-induced block increased under conditions of repetitive stimulation, i.e., rupatadine-induced block was use-dependent, which provides further evidence for the proposed open channel interaction.

The blockade of hKv1.5 channels produced by antiarrhythmic drugs and local anaesthetics share a common mechanism, which in turn is similar to that of internal tetraethylammonium (TEA) and its derivatives, collectively called quaternary ammonium (QA) compounds (Armstrong, 1971; Snyders *et al*., 1992; Snyders & Yeola, 1995). In summary, the cationic form of these drugs blocks the ionic current only after channel opening by binding at a site in the internal mouth of the ionic pore. Further studies have demonstrated that binding of these drugs is determined by an electrostatic component reflecting the electrical binding distance and a hydrophobic component that determines the affinity (Snyders & Yeola, 1995). Application of the Woodhull model (Woodhull, 1973) indicated that this electrostatic component of block was identical for all these drugs, and that it was consistent with a binding reaction sensing 20% of the transmembrane electrical field (fractional electrical distance $\delta = 0.18$ since $z = +1$ for these drugs). Rupatadine induced block was also voltage-dependent but its voltage-dependence was exactly a mirror image of the voltage-dependence exhibited in the presence of cationic drugs. To explain this effect on the basis of a Woodhull model would require $z = -1$ (Woodhull, 1973), which does not apply to rupatadine which predominates in its neutral form at the physiological pH (assuming an internal binding site). Moreover, rupatadine modified the voltage-dependence of hKv1.5 channels activation, so that channels activated at more negative potentials and activation did not reach saturation exhibiting a shallow phase at depolarized membrane potentials. Considering the proposed gating model for hKv1.5 channels ($C \rightleftarrows C \rightleftarrows \ldots \rightleftarrows C \rightleftarrows O_1 \rightleftarrows O_2 \rightleftarrows I_1 \rightleftarrows I_2$) (Rich & Snyders, 1998), the voltage-dependent unblock as well as the second shallow component of the activation curve can be explained under the assumption of a fast selective block of the first open state (O_1) followed by a very fast unblock from the second open state (O_2) of the channel which appeared at more positive potentials. Another possible explanation that can account for the voltage-dependent unblock is that neutral drugs may exhibit a binding site coupled to some voltage-dependent process, such as conformational changes in the pore with potential or movement of the voltage sensor which can sense the transmembrane voltage change (Zhang *et al*., 1997). Recent evidences indicated that the open probability (P_o) for the hKv1.5 channel does not saturate at potentials positive to 0 mV, but undergoes further changes at more positive potentials (Fedida, 1997). Thus, it is possible that such changes could alter the conformation of open channels and confer voltage-dependence to block by an uncharged drug. Another possible explanation is that rupatadine binds to an external site and blocks the channel. Thus, at more positive voltages, K^+ permeation increases and hinders the binding of rupatadine to its external site with a resultant relief of block. Such a mechanism has been proposed to explain the nifedipine-induced block of hKv1.5 channels (Zhang *et al*., 1997). To examine this possibility the $[K^+]_i$ was reduced to 25%. Under these conditions the voltage-dependent unblock induced by rupatadine was abolished. Moreover, the activation curve of hKv1.5 channels in the presence of rupatadine reached saturation, i.e., did not exhibit two components and only the shift of the curve to more negative potentials was apparent. These results suggest that the second shallow component of the activation curve and the voltage-dependent unblock that appeared in the presence of rupatadine at normal $[K^+]_i$ was due to the unblock produced by the K^+ efflux at positive potentials and confirmed and extended previous evidence indicating the existence of an external binding site on hKv1.5 channels (Zhang *et al*., 1997; Delpón *et al*., 1999a).

In an attempt to localize the possible residue involved in this external binding site we studied the effects of rupatadine on R485Y channels. R485 is located at the external entryway of the pore, and represents the equivalent residue to 449 on *Shaker* channels which determines external tetraethylammonium sensitivity (MacKinnon & Yellen, 1990) and C-type inactivation rate (López-Barneo *et al*., 1993). In this mutant channel the voltage-dependent unblock was also abolished indicating that this residue may be involved in the external binding site of rupatadine. However, the total amount of block was not significantly modified and the activation curve of R485Y channels in the presence of rupatadine still exhibited two components. Site-directed mutagenesis confirmed that the midsection of the S6 segment is implicated in the internal binding site for tertiary amine local anaesthetics and antiarrhythmic drugs on hKv1.5 channels (Yeola *et al*., 1996; Franqueza *et al*., 1997). Thus, it is possible that rupatadine also binds to this internal binding site and that its effects on voltage-dependence of hKv1.5 channels activation were not completely due to the unblock produced by the K^+ efflux at positive potentials. In order to test this hypothesis, we performed experiments on V512M channels, a residue that is critical in the stereoselective binding of bupivacaine on hKv1.5 channels (Franqueza *et al*., 1997). V512M mutation shifted $\approx$20 mV the voltage-dependence of channel activation in the negative direction and rupatadine-induced block also exhibited a marked voltage-dependent unblock.

Taking all these results together we proposed the existence of an external and an internal binding site for rupatadine on hKv1.5 channels. Rupatadine blocked in a concentration-, time- and use-dependent manner hKv1.5 channels and it dramatically changed the channel *gating* properties as reflected by the changes induced in the voltage-dependence of channel activation. Moreover, unbinding from the external site

produced by the K^+ efflux is responsible for the voltage-dependent unblock.

This study was supported by SAF96-0042, SAF98-0058, SAF99-0069 and CAM (08.4/0016.1998) Grants. The authors thank Dr M.M. Tamkun and D.J. Snyders for providing the cell line transfected with the gene encoding hKv1.5 channels. We also want to express our thanks to T. González and to Dr M.I. Loza for their constructive criticism of the manuscript. We thank Guadalupe Pablo for her technical assistance.

References

ARMSTRONG, C.M. (1971). Interaction of tetraethylammonium ion derivatives with the potassium channels of giant axons. *J. Gen. Physiol.,* **58,** 413 – 437.

BERUL, C.I. & MORAD, M. (1995). Regulation of potassium channels by nonsedating antihistamines. *Circulation,* **91,** 2220 – 2225.

BRAQUET, P., TOUQUI, L., SHEN, T. & VARGAFTIG, B. (1987). Perspectives in platelet-activating factor research. *Pharmacol. Rev.,* **39,** 97 – 145.

CABALLERO, R., DELPÓN, E., VALENZUELA, C., LONGOBARDO, M., FRANQUEZA, L. & TAMARGO, J. (1997). Effect of descarboethoxyloratadine, the major metabolite of loratadine, on the human cardiac potassium channels Kv1.5. *Br. J. Pharmacol.,* **122,** 796 – 798.

CARCELLER, E., MERLOS, M., GIRAL, M., BALSA, D., ALMANSA, C., BARTROLI, J., GARCIA RAFANELL, J. & FORN, J. (1994). [(3-Pyridylalkyl) piperidylidene] - benzocycloheptapyridine derivatives as dual antagonists of PAF and histamine. *J. Med. Chem.,* **37,** 2697 – 2703.

CARMELIET, E. (1993). Use-dependent block and use-dependent unblock of the delayed rectifier K^+ current by almokalant in rabbit ventricular myocytes. *Circ. Res.,* **73,** 857 – 868.

CRUMB, W.J., WIBLE, B., ARNOLD, D.J., PAYNE, J.P. & BROWN, A.M. (1995). Blockade of multiple human cardiac potassium currents by the antihistamine terfenadine: possible mechanism for the terfenadine-associated toxicity. *Mol. Pharmacol.,* **47,** 181 – 190.

DELPÓN, E., CABALLERO, R., VALENZUELA, C., LONGOBARDO, M., SNYDERS, D. & TAMARGO, J. (1999a). Benzocaine enhances and inhibits the K^+ current through a human cardiac cloned channel (Kv1.5). *Cardiovasc. Res.,* **42,** 510 – 520.

DELPÓN, E., CABALLERO, R., VALENZUELA, C., LONGOBARDO, M., TAMARGO, J. (1998). Direct effects of losartan and its active metabolite on a human cardiac cloned potassium channel (Kv1.5). *Br. J. Pharmacol.,* **124,** 114P.

DELPÓN, E., VALENZUELA, C., GAY, P., FRANQUEZA, L., SNYDERS, D.J. & TAMARGO, J. (1997). Block of human cardiac Kv1.5 channels by loratadine: voltage-, time- and use-dependent block at concentrations above therapeutic levels. *Cardiovasc. Res.,* **35,** 341 – 350.

DELPÓN, E., VALENZUELA, C. & TAMARGO, J. (1999b). Blockade of cardiac potassium and other channels by antihistamines. *Drug Safety,* (in press).

FEDIDA, D. (1997). Gating charge and ionic currents associated with quinidine block of human Kv1.5 delayed rectifier channels. *J. Physiol.,* **499,** 661 – 675.

FRANQUEZA, L., LONGOBARDO, M., VICENTE, J., DELPÓN, E., TAMKUN, M.M., TAMARGO, J., SNYDERS, D.J. & VALENZUELA, C. (1997). Molecular determinants of stereoselective bupivacaine block of hkv1.5 channels. *Circ. Res.,* **81,** 1053 – 1064.

GARCÍA RAFANELL, J. (1996). Rupatadine fumarate. *Drugs Fut.,* **21,** 1032 – 1036.

HANAHAN, D. (1986). Platelet activating factor: a biologically active phosphoglyceride. *Ann. Rev. Biochem.,* **55,** 483 – 509.

KOLTAI, M., HOSFORD, D., GUINOT, P., ESANU, A. & BRAQUET, P. (1991). Platelet-activating factor (PAF): a review of its effect, antagonists and future clinical implications. *Drugs,* **42,** 174 – 204.

LACERDA, A., ROY, M.-L., LEWIS, E.W. & RAMPE, D. (1997). Interactions of the nonsedating antihistamine loratadine with Kv1.5-type potassium channel cloned from human heart. *Mol. Pharmacol.,* **52,** 314 – 322.

LONGOBARDO, M., DELPÓN, E., CABALLERO, R., TAMARGO, J. & VALENZUELA, C. (1998). Structural determinants of potency and stereoselective block of hKv1.5 channels induced by local anesthetics. *Mol. Pharmacol.,* **54,** 162 – 169.

LÓPEZ-BARNEO, J., HOSHI, T., HEINEMANN, S.H. & ALDRICH, R.W. (1993). Effects of external cations and mutations in the pore region on C-type inactivation of *Shaker* potassium channels. *Receptors Channels,* **1,** 61 – 71.

MACKINNON, R. & YELLEN, G. (1990). Mutations affecting TEA blockade and ion permeation in voltage-activated K^+ channels. *Science,* **250,** 276 – 279.

MCINTYRE, T., ZIMMERMAN, G., SATOH, K. & PRESCOTT, S.M. (1985). Cultured endothelial cells synthesize both platelet-activating factor and prostacyclin in response to histamine, bradykinin and adenosine triphosphate. *J. Clin. Invest.,* **76,** 271 – 280.

MERLOS, M., GIRAL, M., BALSA, D., FERRANDO, R., QUERALT, M., PUIGDEMONT, A., GARCÍA-RAFANELL, J. & FORN, J. (1997). Rupatadine, a new potent, orally active dual antagonist of histamine and platelet-activating factor (PAF). *J. Pharmacol. Exp. Ther.,* **280,** 114 – 121.

PRESSCOTT, S.M., ZIMMERMAN, G.A. & MCINTYRE, T.M. (1987). The production of platelet-activating factor by cultured human endothelial cells: regulation and function. In *Platelet-activating factor and related lipid mediators.* Snyder, F. ed. pp. 323 – 340. New York: Plenum Press.

RAMPE, D., WIBLE, B., BROWN, A. & DAGE, R.G. (1993). Effects of terfenadine and its metabolites on a delayed rectifier K^+ channel cloned from human heart. *Mol. Pharmacol.,* **44,** 1240 – 1245.

RICH, T.C. & SNYDERS, D.J. (1998). Evidence for multiple open and inactivated states of the hKv1.5 delayed rectifier. *Biophys. J.,* **75,** 183 – 195.

SALATA, J.J., JURKIEWICZ, N.K., WALLACE, A.A., STUPIENSKI, R.F., GUINOSSO, P.J. & LYNCH, J.J. (1995). Cardiac electrophysiological actions of the histamine H_1-receptor antagonists astemizole and terfenadine compared with chlorpheniramine and pyrilamine. *Circ. Res.,* **76,** 110 – 119.

SCHWARTZ, L. (1994). Mast cells: functions and contents. *Curr. Opin. Immunol.,* **6,** 91 – 97.

SCIBERRAS, D.G., BOLOGNESE, J.A., GOLDENBERG, M.M., JAMES, I. & BABER, N.S. (1988). Platelet-activating factor induced inflammatory responses in the skin. *Prostaglandins,* **35,** 833. (abstract).

SERAFIN, W. & AUSTEN, K. (1987). Mediators of immediate hypersensitivity reactions. *N. Engl. J. Med.,* **317,** 30 – 34.

SIMONS, F.E.R. & SIMONS, K.J. (1991). Pharmacokinetic optimisation of histamine H_1-receptor antagonist therapy. *Clin. Pharmacokin.,* **21,** 372 – 393.

SNYDERS, D., KNOTH, K., ROBERDS, S. & TAMKUN, M.M. (1992). Time-, state- and voltage-dependent block by quinidine of a cloned human cardiac channel. *Mol. Pharmacol.,* **41,** 332 – 339.

SNYDERS, D., TAMKUN, M.M. & BENNETT, P.B. (1993). A rapidly activating and slowly inactivating potassium channel cloned from human heart. *J. Gen. Physiol.,* **101,** 513 – 543.

SNYDERS, D.J. & YEOLA, S.W. (1995). Determinants of antiarrhythmic drug action: electrostatic and hydrophobic components of block of the human cardiac hKv1.5 channel. *Circ. Res.,* **77,** 575 – 583.

TSENG, G.-N., ZHU, B., LING, S. & YAO, J.-A. (1996). Quinidine enhances and suppresses Kv1.2 from outside and inside the cell, respectively. *J. Pharmacol. Exp. Ther.,* **279,** 844 – 855.

VALENZUELA, C., DELPÓN, E., FRANQUEZA, L., GAY, P., PÉREZ, O., TAMARGO, J. & SNYDERS, D.J. (1996). Class III antiarrhythmic effects of zatebradine. Time-, state-, use-, and voltage-dependent block of hKv1.5 channels. *Circulation,* **94,** 562 – 570.

VALENZUELA, C., DELPÓN, E., FRANQUEZA, L., GAY, P., VICENTE, J. & TAMARGO, J. (1997). Comparative effects of nonsedating histamine H_1 receptor antagonists, ebastine and terfenadine, on human Kv1.5 channels. *Eur. J. Pharmacol.,* **326,** 257 – 263.

WANG, Z., FERMINI, B. & NATTEL, S. (1993). Sustained depolarization-induced outward current in human atrial myocytes. Evidence for a novel delayed rectifier K^+ current similar to Kv1.5 cloned channel currents. *Circ. Res.,* **73,** 1061 – 1076.

WEILAND, G. & MOLINOFF, P. (1981). Quantitative analysis of drug-receptor interactions: I. Determination of kinetic and equilibrium properties. *Life Sci.,* **29,** 313 – 330.

WOODHULL, A.M. (1973). Ionic blockage of sodium channels in nerve. *J. Gen. Physiol.,* **61,** 687 – 708.

YEOLA, S.W., RICH, T.C., UEBELE, V.N., TAMKUN, M.M. & SNYDERS, D.J. (1996). Molecular analysis of a binding site for quinidine in a human cardiac delayed rectifier K^+ channel. Role of S6 in antiarrhythmic drug binding. *Circ. Res.,* **78,** 1105 – 1114.

ZHANG, X., ANDERSON, J.W. & FEDIDA, D. (1997). Characterization of nifedipine block of the human heart delayed rectifier, hKv1.5. *J. Pharmacol. Exp. Ther.,* **281,** 1247 – 1256.

(Received April 7, 1999
Revised July 19, 1999
Accepted August 18, 1999)